

# Development and validation of a LRP1B mutation-associated prognostic model for hepatocellular carcinoma

Jian Xu (✉ [58364386@qq.com](mailto:58364386@qq.com))

Tianjin City Second People's Hospital <https://orcid.org/0000-0002-1359-9820>

**Xiaomin Shen**

Tianjin City Second People's Hospital

**Bo Zhang**

Tianjin Medical University

**Rui Su**

Tianjin City Second People's Hospital

**Mingxuan Cui**

Tianjin Medical University

**Li Yan**

Tianjin City Second People's Hospital

**Yu Cao**

Tianjin City Second People's Hospital

---

## Primary research

**Keywords:** hepatocellular carcinoma, LRP1B, prognostic model, immune cell infiltration ratio, immune checkpoint

**Posted Date:** May 3rd, 2021

**DOI:** <https://doi.org/10.21203/rs.3.rs-266054/v1>

**License:**  This work is licensed under a Creative Commons Attribution 4.0 International License.

[Read Full License](#)

---

**Version of Record:** A version of this preprint was published at Bioscience Reports on August 31st, 2021. See the published version at <https://doi.org/10.1042/BSR20211053>.

# Abstract

**Purpose:** To develop a LRP1B gene mutation based prognostic model for hepatocellular carcinoma (HCC) patients risk prediction.

**Methods:** The LRP1B gene mutation rate was calculated from HCC patient samples. Meanwhile, differentially expressed genes according to LRP1B mutant were screened out for prognostic model establishment. Based on this innovative model, HCC patients were categorized into high and low-risk group. The immune status including immune cell infiltration ratio and checkpoints have been explored in two groups.

**Results:** It can be shown here 11 genes demonstrate significant differences according to LRP1B status, which can better predict HCC patient prognosis. The accuracy of the model prediction is evaluated and approved by the AUC value. From the immune cell infiltration ratio analysis, there is a significant difference in the infiltration degree of 7 types of immune cells and 2 immune checkpoints between high and low-risk HCC patients. Meanwhile, LRP1B was tested as a prognostic marker in clinic to predict different stages for HCC with satisfied accuracy.

**Conclusion:** This study has explored a potential prognostic biomarker and developed a novel LRP1B mutation-associated prognostic model for hepatocellular carcinoma, which provides a systematic reference for future better understanding of clinical research.

## Background

Hepatocellular Carcinoma (HCC) is the fourth most abundant malignant tumor in the world as well as the second leading cause for the cancer-related human deaths, accounting for nearly 841,000 new cases and 782,000 deaths annually<sup>[1]</sup>. In the aspect of virus infection, the hepatitis B virus (HBV) and hepatitis C virus (HCV) are the critical causes for HCC development<sup>[2]</sup>. In addition to the viral hepatitis from HBV and HCV, there are still some non-viral risk factors that can induce the development of HCC<sup>[3]</sup>. Diabetes mellitus, alcohol abuse, cardiovascular disease, liver inflammation, obesity, dyslipidemia and non-alcoholic fatty liver disease (NAFLD) are some other major contributors to HCC development<sup>[4-6]</sup>. Although the prospects for better diagnosis and treatments of HCC have dramatically improved over the past decade, an comprehensive understanding of the pathogenesis of HCC remains a substantial impediment.

LRP1B represents lipoprotein receptor-related protein 1B gene, which has been initiated as a new tumor suppressor candidate gene<sup>[7]</sup>. It may inhibit tumor cell infiltration and metastasis by antagonizing the extracellular UPA system to hydrolyze proteins, degrading EMC, and preventing cell movement<sup>[8]</sup>. Studies have found that changes in the gene cause nearly 40% of the non-small cell lung cancer cell line<sup>[9]</sup>. At the same time, it was suggested that LRP1B was down-regulated in colon cancer tissues and suppressed the cell proliferation, migration and metastasis of colon cancer cells, which is closely associated with beta-

catenin/TCF signaling<sup>[10]</sup>. Taken together, several studies have demonstrated the suppressive roles of LRP1B in the cancer progression, implicating that restoring the function of LRP1B would be a promising strategy for the cancer treatment. However, the relation between LRP1B and HCC is still poorly understood.

Based on the fact of poor accuracy of prognosis, the HCC has brought great difficulty to clinical treatment. Since LRP1B has attracted more and more attention in the cancer research currently, a more comprehensive approach to build a LRP1B mutation-associated prognostic model for HCC is required. To address these issues, in this study, the mutation rate of LRP1B in HCC patients and differentially expressed genes have been investigated deeply by a combination of bioinformatics and machine learning method to build a innovative HCC prognostic model. Moreover, the 22 specific immune cell infiltration as well as 6 immune checkpoints in LRP1B mutated HCC have been also studied comprehensively. All of these promising outcomes enriched the precise prognosis of the disease, which provide tremendous help for future HCC study.

## Material And Methods

### *Data Source*

We downloaded the MAF file for mutation information of 365 HCC patients from the database: **The Cancer Genome Atlas** (TCGA, <https://tcga-data.nci.nih.gov/tcga/>), of which 357 patients had complete survival information, which was used for the following analysis. In addition, we also obtained 237 HCC patients with complete clinical as well as mRNA expression information from ICGC database (<https://icgc.org/>), numbered Liver Cancer-RIKEN, JP (LIRI-JP).

### *LASSO Cox regression analysis*

Based on the expression values of differentially expressed genes, the Cox regression analysis was developed on the HCC samples, while the genes that are significantly related to the prognosis of HCC were screened with a threshold of  $P < 0.01$ . Then the glmnet package of R language was generated for LASSO Cox regression analysis in order to further select the genes associated with the prognosis of HCC<sup>[11]</sup>. The selected genes were established for risk score based on the following formula:

$$\text{Risk score} = \sum_{i=1}^n \text{Coef}_i * x_i,$$

Then the patients were divided into high-risk group and low-risk group according to the median of the risk score.

### *Survival analysis*

The survival analysis was performed using the R language survival package and survminer (<https://CRAN.R-project.org/package=survminer>). The package estimates the overall survival rate of different TCGA groups based on the Kaplan-Meier method, and uses log-rank test to investigate the significance of survival difference between different groups.

### ***Differential gene analysis***

The differentially expressed genes analysis were based on the limma function package<sup>[12]</sup> of the R language (version 3.5.2), with the difference factor greater than 1.5 times and  $FDR \leq 0.05$  as a criteria.

### ***Calculation of immune cell infiltration ratio***

The software CIBERSORT was utilized to calculate the relative proportion of 22 immune cells in HCC patients<sup>[13]</sup>. The CIBERSORT software could use the deconvolution algorithm with the preset 547 barcodes to characterize the composition of immune infiltrating cells according to the gene expression matrix.

### ***LRP1B clinical examination***

Subjects were retrospectively analyzed from January 2017 to December 2019 pathologically for HCC stage confirmation. Patients were classified according to the latest standards, which was the actual stage of the patient.

### ***LRP1B concentration detection with ELISA method***

LRP1B concentration determination adopted ELISA double antibody sandwich method, the specific operation was strictly carried out in accordance with the kit instructions (Abcam company): the sample was extracted from peripheral blood of HCC patients. The results of the determination were repeated three times. The prognostic stage of HCC patients was determined according to LRP1B concentration, which was the forecast staging.

### ***Statistical analysis***

The multi-factor Cox regression model was developed to analyze whether risk score could predict the survival of patients with HCC independently. The Wilcoxon signed rank sum test method was used to compare the differences of immune cell infiltration. The statistical analysis was established by R software, with version number v3.5.2.

## **Results**

### ***HCC patients with mutations in LRP1B have a worse prognosis***

The mutation rate of LRP1B gene is high in TCGA patients with HCC, ranking at the 13th place, reaching about 8% (Figure 1A), and the overall survival of LRP1B mutant HCC patients is significantly lower than that of LRP1B wild-type HCC patients (Figure 1B). Then we analyzed the differentially expressed genes of

LRP1B mutant and wild-type HCC patients, concluding that 187 genes demonstrate specific expression manner in LRP1B mutant HCC patients. There were 134 up-regulated genes and 53 down-regulated genes shown as Figure 1C and Figure 1D.

### ***The risk model constructed by 11 genes can better predict the prognosis of HCC patients***

Univariate Cox regression analysis was performed with 187 differentially expressed gene as continuous variables. At the same time, the Hazard ratio (HR) of each gene was calculated. With P-value < 0.01 as the threshold, 68 genes were finally selected out. Protective genes with HR value less than 1 were favorable for prognosis, while risk genes with HR value greater than 1 were unfavorable for prognosis. It was turned out that 3 of the 68 genes were protective genes, and the remaining 65 genes were risk genes. The forest map of the top 20 genes with the smallest P-value among these 68 genes is shown in Figure 2A. The optimal number of genes was 11 (Figure 2B, with the smallest lambda value), 11 genes were CELSR3, KLRB1, CENPA, CDCA8, PKIB, ADAMTS5, FTCD, CDX2, SFN, MYT1L and ZP3, respectively.

The risk score model was established for predicting survival:  $\text{Risk score} = (0.019437033 * \text{CELSR3}) + (-0.138416034 * \text{KLRB1}) + (0.070137596 * \text{CENPA}) + (0.093717620 * \text{CDCA8}) + (0.007794412 * \text{PKIB}) + (0.166654021 * \text{ADAMTS5}) + (-0.041895786 * \text{FTCD}) + (0.054670700 * \text{CDX2}) + (0.006845825 * \text{SFN}) + (0.026858059 * \text{MYT1L}) + (0.047343209 * \text{ZP3})$ . We calculated the risk score for each patient and divided the TCGA data set and the ICGC validation set into the high-risk group and the low-risk group according to the median of the risk score.

Survival analysis showed that in TCGA data set and ICGC validation set, the high-risk HCC samples had the worse overall survival (Figure 2C). In addition, the AUC of 1-year, 3-year and 5-year survival time of TCGA dataset was 0.8119, 0.7622 and 0.7001 respectively (Figure 2D). The AUC of 1-year, 3-year and 5-year survival in ICGC validation set were 0.7182, 0.7297 and 0.7545 respectively, which indicated that the risk model could predict the prognosis of HCC patients effectively in both datasets. At the same time, we found that the expression of 11 genes was significantly different between high-risk and low-risk groups in TCGA and ICGC dataset (Figure 2E). In general, the risk score calculated from the risk model constructed by Celsr3, Klr1b1, CENPA, CDCA8, PKIB, Adamts5, FTCD, CDX2, SFN, MYT1L and ZP3 could predict the prognosis of patients with HCC.

### ***Risk score is an independent prognostic marker of HCC***

We included age, sex, stage, LRP1B status, HBV index, and risk score for the next investigation. The results are shown in Figure 3A. It was found that risk score and age were significantly associated with overall survival, and the samples with high risk score had a higher risk of death and were unfavorable for prognosis (HR=3.24, 95% CI: 2.26-4.6,  $P < 0.001$ ).

In order to further explore the prognostic value of risk score in HCC patients with different clinicopathological factors (including age and stage), we regrouped patients by age and stage, performing a Kaplan-Meier survival analysis. It could be demonstrated that the overall survival rate of the high-risk group is clearly lower than that of the low-risk group of the samples in different ages and stages

(Figure 3B-3C). These results confirm that the risk score can be used as an independent indicator to predict the prognosis for HCC patients.

### ***Nomogram model can better predict the prognosis of HCC patients***

We use four independent prognostic factors: age, gender, radiotherapy status as well as risk score to construct the nomogram model (Figure 4A). For each patient, draw three lines upwards to determine the points obtained from each factor in the Nomogram. The "Total Points" axis is determined by the sum of these points, of which draw a line to generate the probability of HCC patients surviving 1, 3, and 5 years. The one-year and two-year corrected curves in the calibration chart are relatively close to the ideal curves (Figure 4B-4D).

### ***Immune status of HCC patients in high and low-risk groups***

We used the CIBERSORT method combined with LM22 feature matrix to estimate the difference of immune infiltration between 22 immune cells in high-risk and low-risk groups of patients with HCC. Figure 5A summarized the results of immune cell infiltration in 352 HCC patients. There are significant differences in the infiltration ratios of 7 types of immune cells, such as Macrophages (M0), between high and low-risk groups (Figure 5B).

Since the expression of immune checkpoints has become a biomarker of immunotherapy for HCC patients, we analyzed the correlation between patient risk score and key immune checkpoints (CTLA4, PDL1, LAG3, TIGIT, IDO1, TDO2). It could be seen that the risk score is closely associated with the 6 checkpoints (Figure 6A). At the same time, 2 of the 6 immune checkpoints (PDL1, TDO2) have the significant differences in the high and low-risk groups of HCC patients (Figure 6B-6C).

### ***LRP1B gene can be used a HCC prognostic marker***

Since the LRP1B gene demonstrate specific expression among different prognostic stages, next we testified whether LRP1B gene could be developed as a clinical marker to predict prognostic stages for HCC (Table 1). The results clearly support that the accuracy rate using LRP1B gene as a HCC prognostic marker reaches the standard.

## **Discussion**

HCC is the most common primary tumor of the liver and its mortality is third among all solid tumors, just behind carcinomas of the lung and the colon<sup>[14-17]</sup>. In this study, we established a innovative prognostic analysis based on LRP1B mutation. First of all, the mutation rate of LRP1B gene in HCC is shown to reaches 8%, which is relatively high among all the mutations. Moreover, majoritory of differentially genes in LRP1B mutation HCC samples are risk genes, which are unfavorable for prognosis. These results are consistent with the function of LRP1B as a potential tumor suppressor. Previously, LRP1B has been studied in lung cancer as well as colon cancer<sup>[18]</sup>. However, its role in HCC is still under contraversial. A

research by Ikari and his colleagues suggests that LRP1B is one of most prominent somatic mutations in liver cancer metastasis, which initiate the key LRP1B function in HCC<sup>[19]</sup>. To this end, using LRP1B as an independent variable, we generated a risk score model aiming for HCC prognostic prediction. The accuracy of the model prediction is evaluated and approved by the AUC value, which demonstrates not only the rationality of our method on the one hand but also the importance of the prediction model for future HCC prognosis.

In addition to the prognosis model establishment for HCC, another feature of this study is to explore multiple key associated genes. Cadherin EGF LAG seven-pass G-type receptor 3 (CELSR3) is the key signaling molecule in the wntless and INT-1/planar cell polarity (WNT/PCP) pathway<sup>[20]</sup>. It has been demonstrated as an organ-, inflammation- and cancer specific transcriptional fingerprint of pancreatic and hepatic stellate cells<sup>[21]</sup>. Moreover, CELSR3 is suggested to be involved in the progression of cancer and can be used as a biomarker for the prognosis of HCC patients directly<sup>[22]</sup>. The killer cell lectin-like receptor B1 (KLRB1) gene encodes for CD161 expressed by different subsets of leukocytes involved in the development of acute liver transplant rejection<sup>[23]</sup>. It has been promoted as a favorably prognostic gene by a pan-cancer resource and meta-analysis of expression signatures from 18,000 human tumors with overall survival outcomes across 39 malignancies<sup>[24]</sup>. CENPA stands for centromere protein A, which is initiated as a novel biomarker not only for HCC but also for lung cancer<sup>[25]</sup>. Altered expression of ADAMTS5 is associated with human carcinogenesis and tumor progression<sup>[26]</sup>. ADAMTS5 has been approved to be expressed at differential levels in hepatocellular carcinoma cell lines, which also plays a role in suppression of HCC progression<sup>[27]</sup>. Beside these, the connection between the other genes and HCC are not clear yet. All of these deserve further investigation.

Here, we also deeply investigate the immune cell infiltration in different groups of HCC patients distinguished by LRP1B mutation, where differences in the proportion of immune cell infiltration may be an intrinsic feature of individual differences receiving immunotherapy. In addition, the correlation between different types of immune cells is weak, which indicates that there is a large heterogeneity in the infiltration of different immune cells in tumor patients. Here, in this study, 7 types of immune cells, such as Macrophages (M0) as well as 2 of the 6 immune checkpoints (PDL1, TDO2) have the significant differences in the high and low-risk groups of HCC patients, indicating that the poor prognosis of HCC patients with high risk may be due to the immunosuppressive microenvironment. Immune checkpoints include stimulatory and inhibitory checkpoint molecules. The programmed cell death 1 ligand 1 (PDL-1) is suggested to function as a inhibitory checkpoint, which was identified to suppress anti-tumor immune responses in solid tumors<sup>[28]</sup>. Currently, several novel drugs targeting immune checkpoints have succeeded in cancer treatment<sup>[29]</sup>. The combination of anti-PD-1/PD-L1 with anti-CTLA-4 antibodies is being evaluated in phase 1, 2 or 3 trials of HCC<sup>[30]</sup>. At the same time, cancer epigenetic modulations of checkpoints also increase our understanding of potential therapeutic targets in related to the tumor microenvironment. Here, we explore the connection between these checkpoints to LRP1B mutant HCC, which represents a high frequency of HCC patients. This may call for a great point for the future study.

To conclude, in the light of the fact that there remains no gold standard prognosis and no reliable disease-specific prediction for HCC, we establish an innovative prognostic model for HCC based on LRP1B mutant patients. According to the model, several related genes and 7 immune cells as well as 2 key immune checkpoints demonstrate significant difference in high and low-risk groups. Overall, we shed light on questions and challenges posed by HCC, and we establish an innovative prediction target which can provide great help for future reference of the disease.

## Declarations

Ethics approval and consent to participate

Not applicable

Consent for publication

Not applicable

Availability of data and materials

The datasets used or analysed during the current study are available from the corresponding author on reasonable request.

Competing interests

The authors declare no competing interests.

Funding

This research was funded by the National Natural Science Foundation of China (Grant NO.82070687 to B.Z.).

Authors' contributions

Haitang Ren and Zheng Luo analyzed the data and contributed equally to the work; Min Wang collected the data; Lei Chen wrote the manuscript; Bo Zhang supervised the work.

Acknowledgements

Not applicable

## References

1. El-Serag HB. 2011. Hepatocellular carcinoma. *The New England journal of medicine* 365:1118-27
2. Forner A, Reig M, Bruix J. 2018. Hepatocellular carcinoma. *Lancet* 391:1301-14

3. Grandhi MS, Kim AK, Ronnekleiv-Kelly SM, Kamel IR, Ghasebeh MA, Pawlik TM. 2016. Hepatocellular carcinoma: From diagnosis to treatment. *Surgical oncology* 25:74-85
4. Golabi P, Rhea L, Henry L, Younossi ZM. 2019. Hepatocellular carcinoma and non-alcoholic fatty liver disease. *Hepatology international* 13:688-94
5. Colquhoun SD. 2016. Hepatocellular Carcinoma: The Current Role of Surgical Intervention. *Critical reviews in oncogenesis* 21:93-103
6. Hartke J, Johnson M, Ghabril M. 2017. The diagnosis and treatment of hepatocellular carcinoma. *Seminars in diagnostic pathology* 34:153-9
7. Chen H, Chong W, Wu Q, Yao Y, Mao M, Wang X. 2019. Association of LRP1B Mutation With Tumor Mutation Burden and Outcomes in Melanoma and Non-small Cell Lung Cancer Patients Treated With Immune Check-Point Blockades. *Frontiers in immunology* 10:1113
8. Ni S, Hu J, Duan Y, Shi S, Li R, et al. 2013. Down expression of LRP1B promotes cell migration via RhoA/Cdc42 pathway and actin cytoskeleton remodeling in renal cell cancer. *Cancer science* 104:817-25
9. Beer AG, Zenzmaier C, Schreinlechner M, Haas J, Dietrich MF, et al. 2016. Expression of a recombinant full-length LRP1B receptor in human non-small cell lung cancer cells confirms the postulated growth-suppressing function of this large LDL receptor family member. *Oncotarget* 7:68721-33
10. Zhang Z, Cui R, Li H, Li J. 2019. miR-500 promotes cell proliferation by directly targetting LRP1B in prostate cancer. *Bioscience reports* 39
11. Friedman J, Hastie T, Tibshirani R. 2010. Regularization Paths for Generalized Linear Models via Coordinate Descent. *Journal of statistical software* 33:1-22
12. Yu G, Wang LG, Han Y, He QY. 2012. clusterProfiler: an R package for comparing biological themes among gene clusters. *Omics : a journal of integrative biology* 16:284-7
13. Newman AM, Liu CL, Green MR, Gentles AJ, Feng W, et al. 2015. Robust enumeration of cell subsets from tissue expression profiles. *Nature methods* 12:453-7
14. Li S, Yang F, Ren X. 2015. Immunotherapy for hepatocellular carcinoma. *Drug discoveries & therapeutics* 9:363-71
15. Kudo M. 2019. Targeted and immune therapies for hepatocellular carcinoma: Predictions for 2019 and beyond. *World journal of gastroenterology* 25:789-807
16. Villanueva A. 2019. Hepatocellular Carcinoma. *The New England journal of medicine* 380:1450-62
17. Waidmann O. 2018. Recent developments with immunotherapy for hepatocellular carcinoma. *Expert opinion on biological therapy* 18:905-10
18. Wang Z, Sun P, Gao C, Chen J, Li J, et al. 2017. Down-regulation of LRP1B in colon cancer promoted the growth and migration of cancer cells. *Experimental cell research* 357:1-8
19. Ikari N, Serizawa A, Mitani S, Yamamoto M, Furukawa T. 2019. Near-Comprehensive Resequencing of Cancer-Associated Genes in Surgically Resected Metastatic Liver Tumors of Gastric Cancer. *The*

American journal of pathology 189:784-96

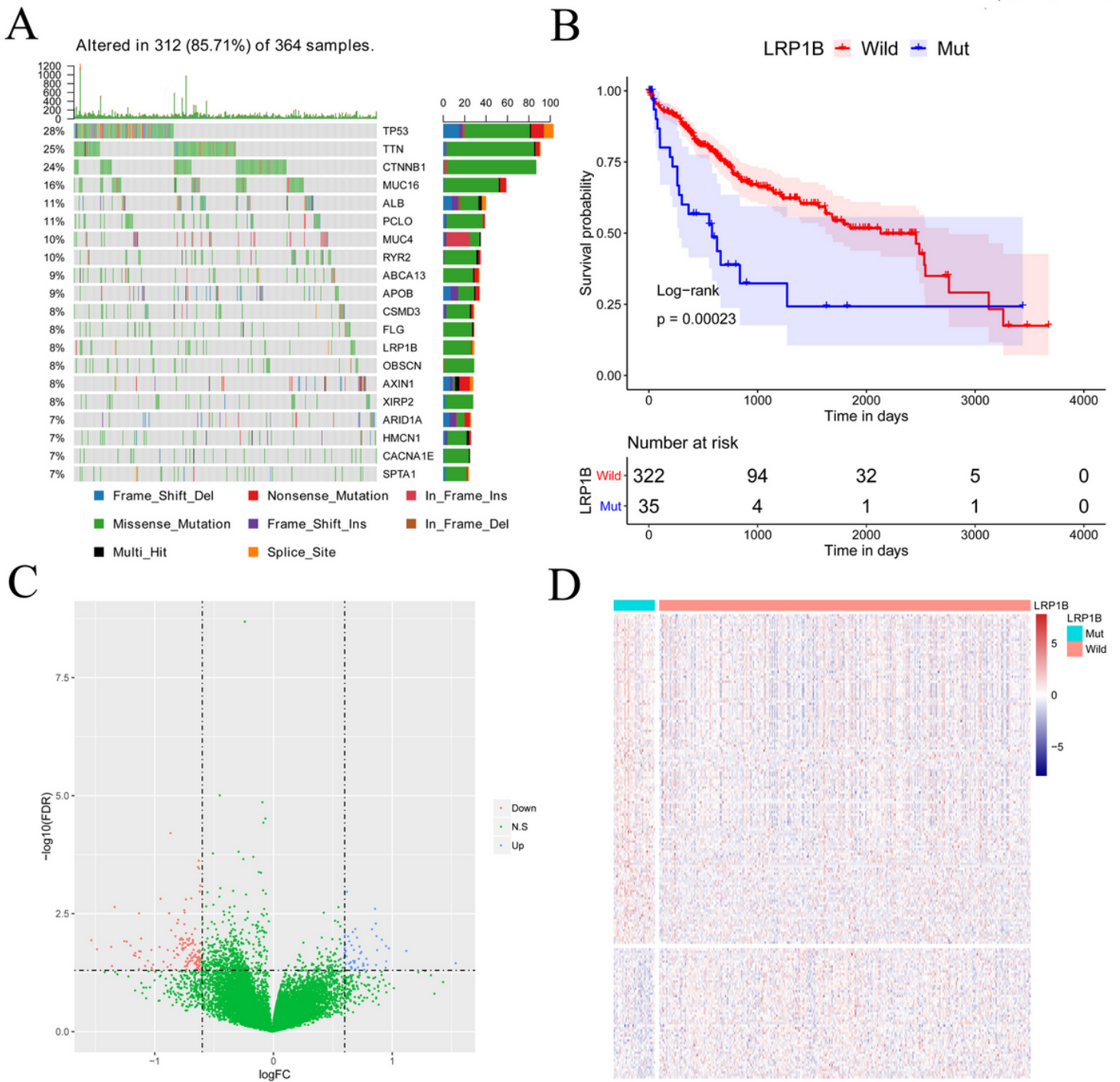
20. Goryca K, Kulecka M, Paziewska A, Dabrowska M, Grzelak M, et al. 2018. Exome scale map of genetic alterations promoting metastasis in colorectal cancer. BMC genetics 19:85
21. Erkan M, Weis N, Pan Z, Schwager C, Samkharadze T, et al. 2010. Organ-, inflammation- and cancer specific transcriptional fingerprints of pancreatic and hepatic stellate cells. Molecular cancer 9:88
22. Gu X, Li H, Sha L, Mao Y, Shi C, Zhao W. 2019. CELSR3 mRNA expression is increased in hepatocellular carcinoma and indicates poor prognosis. PeerJ 7:e7816
23. Thude H, Rother S, Sterneck M, Klempnauer J, Nashan B, et al. 2018. The killer cell lectin-like receptor B1 (KLRB1) 503T>C polymorphism (rs1135816) and acute rejection after liver transplantation. Hla 91:52-5
24. Liu WT, Wang Y, Zhang J, Ye F, Huang XH, et al. 2018. A novel strategy of integrated microarray analysis identifies CENPA, CDK1 and CDC20 as a cluster of diagnostic biomarkers in lung adenocarcinoma. Cancer letters 425:43-53
25. Turner SL, Mangnall D, Bird NC, Bunning RA, Blair-Zajdel ME. 2012. Expression of ADAMTS-1, ADAMTS-4, ADAMTS-5 and TIMP3 by hepatocellular carcinoma cell lines. International journal of oncology 41:1043-9
26. Xu H, Wang H, Zhao N, Zhou F, Yang J. 2016. Lipid deposition in liver cells: The influence of short form augments liver regeneration. Clinics and research in hepatology and gastroenterology 40:186-94

## Table

**Table 1** Detection of prognosis stage of HCC using LRP1B as a marker [case]

Group	TNM Stage I forecast/actual	TNM Stage II forecast/actual	TNM Stage III forecast/actual	TNM Stage IV forecast/actual
LRP1B	41 /37	32/36	22/24	25/23
Accuracy	90.2%	88.9%	91.7%	92.0%

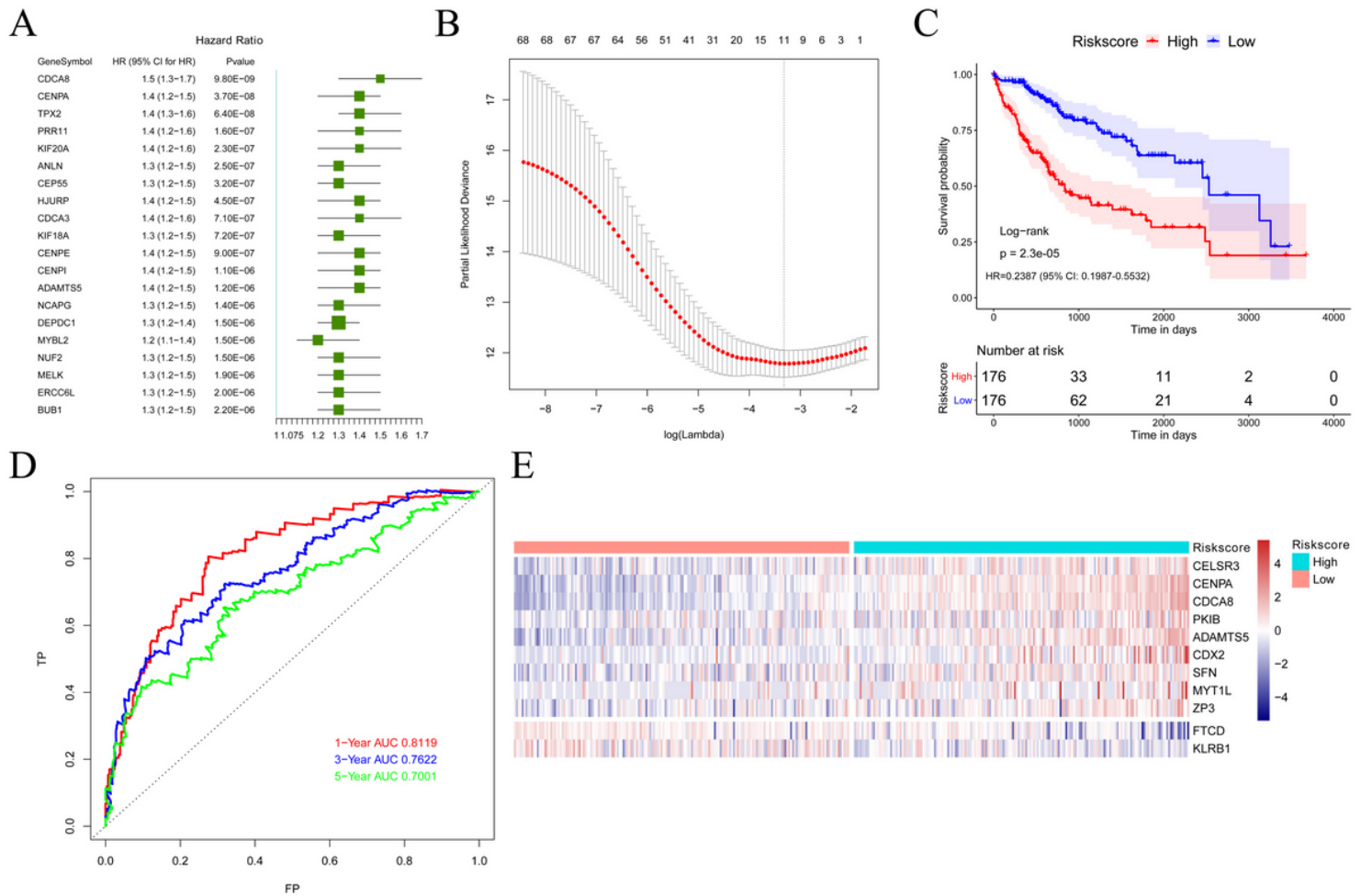
## Figures



**Figure 1**

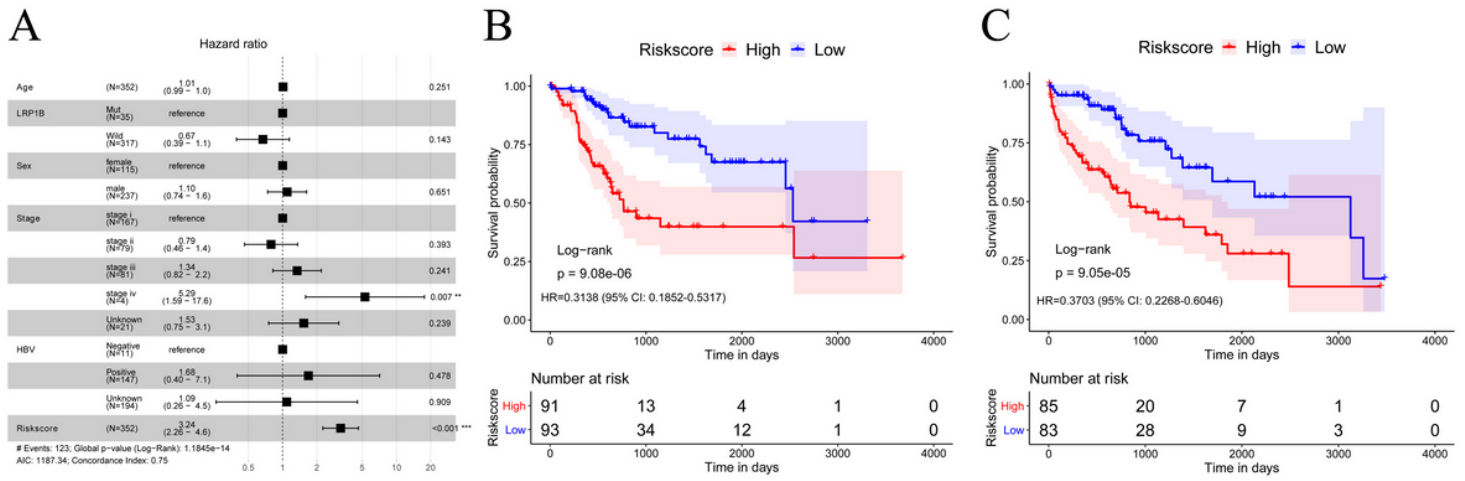
LRP1B mutation status is significantly related to prognosis. (A) Waterfall plot of the top 20 genes with the highest liver cancer mutation rate in the TCGA sample. (B) Kaplan Meier survival curve. The horizontal axis is time, the vertical axis is survival rate respectively. Different colors represent different groups. The P-value is calculated based on the log-rank test. (C) The volcano map of differentially expressed genes. The horizontal axis is the differential expression fold ( $\log_2(\text{FC})$ ), while the vertical axis is  $-\log_{10}(\text{FDR})$  respectively. The blue dots indicate the up-regulated genes, and the red dots indicate the down-regulated genes. (D) Heat map of differentially expressed genes. The horizontal axis is the sample, the vertical axis

is the different genes. At the same time, red indicates high gene expression, blue indicates low gene expression.



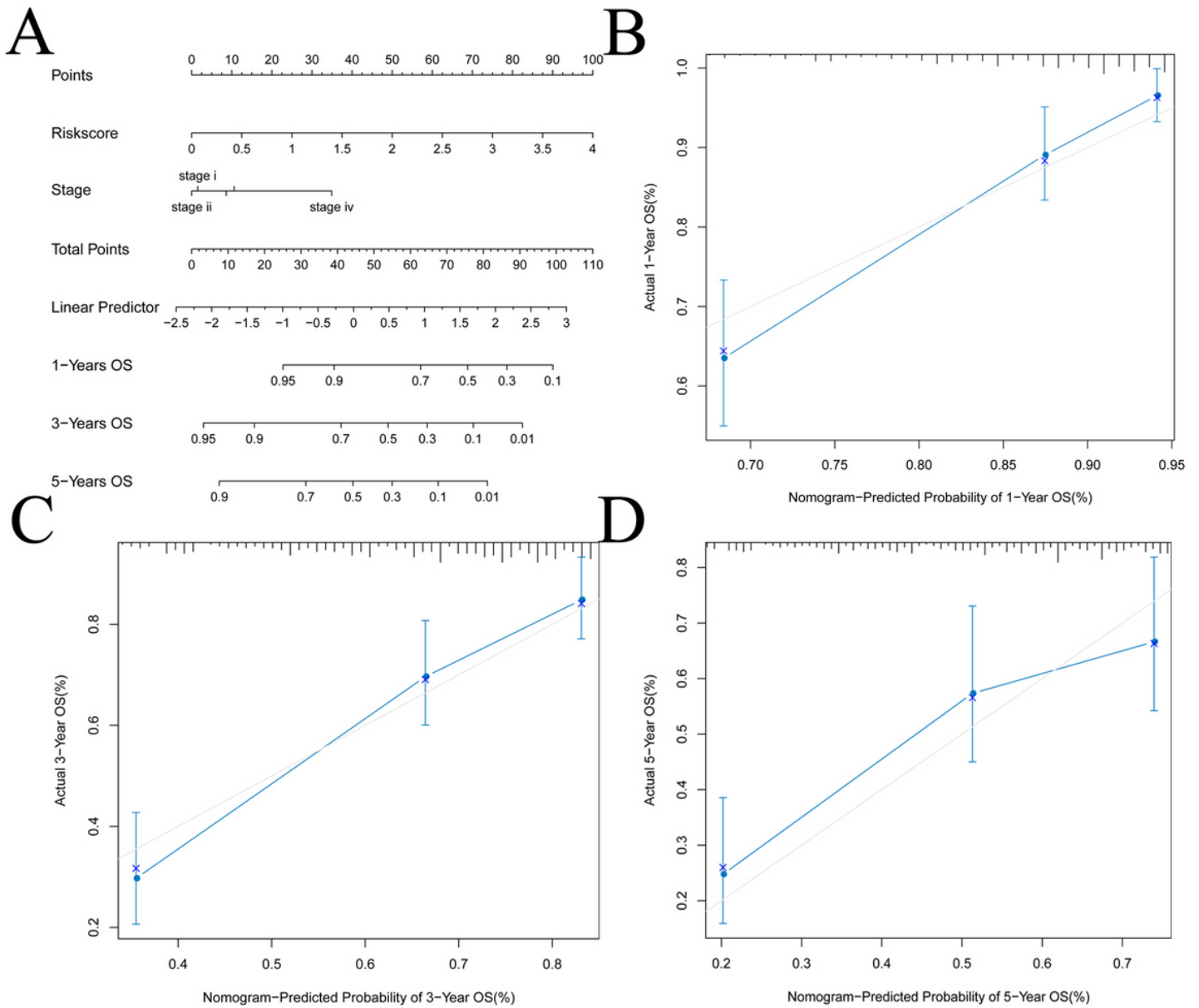
**Figure 2**

Construction of a prognostic model of HCC. (A) Forest plot of the single factor analysis of the top 20 most significant genes related to the prognosis of HCC. HR is Hazard ratio, 95% CI is 95% confidence interval. (B) The graph of determining the tuning parameter lambda in the LASSO regression model. The horizontal axis is log (lambda), and the vertical axis is the partial likelihood deviation value respectively. The lambda value corresponding to the smallest value is the best, which means that the best lambda value after Log is taken below the dotted line, and the number above is the number of variables. (C) Kaplan Meier survival curve in the TCGA data set, the horizontal axis is time, the vertical axis is survival rate. Different colors represent different groups. The P value is based on the log-rank test. (D) The time-dependent roc curve, false positive on the horizontal axis and true positive on the vertical axis were used to estimate the AUC (area under the ROC curve) . (E) The calorimetric maps of the mRNA expression of the 11 selected genes in the high and low-risk score samples of TCGA data set. The horizontal axis indicates the sample while the vertical axis indicates the gene. Meanwhile the red represents the high expression, the blue represents the low expression respectively. The categories of the samples are marked with different colors above the heat map.



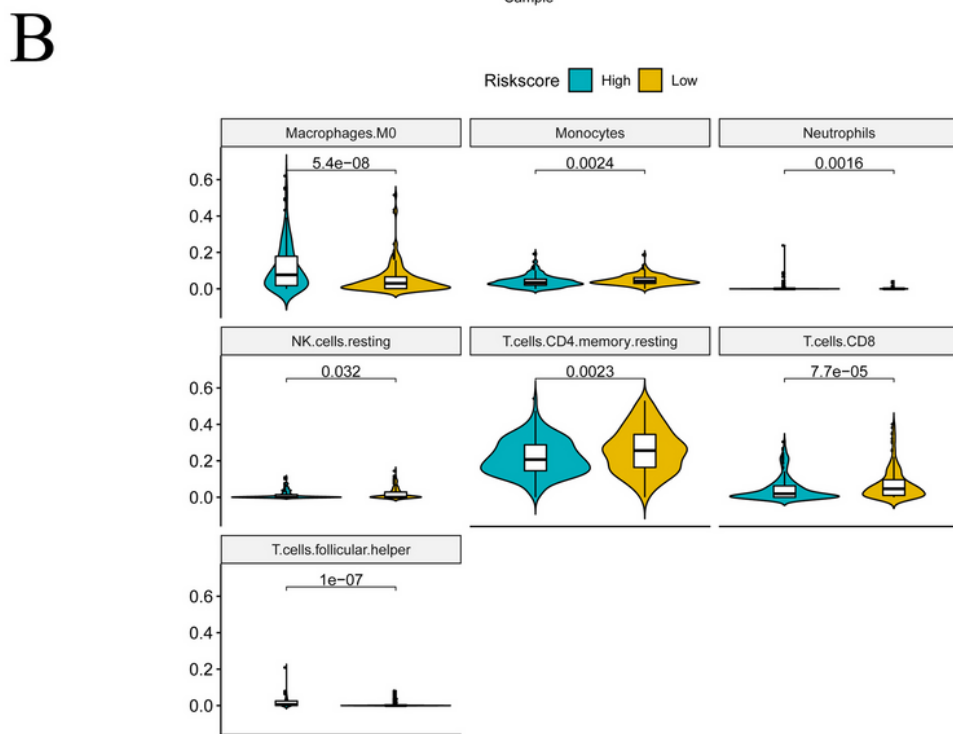
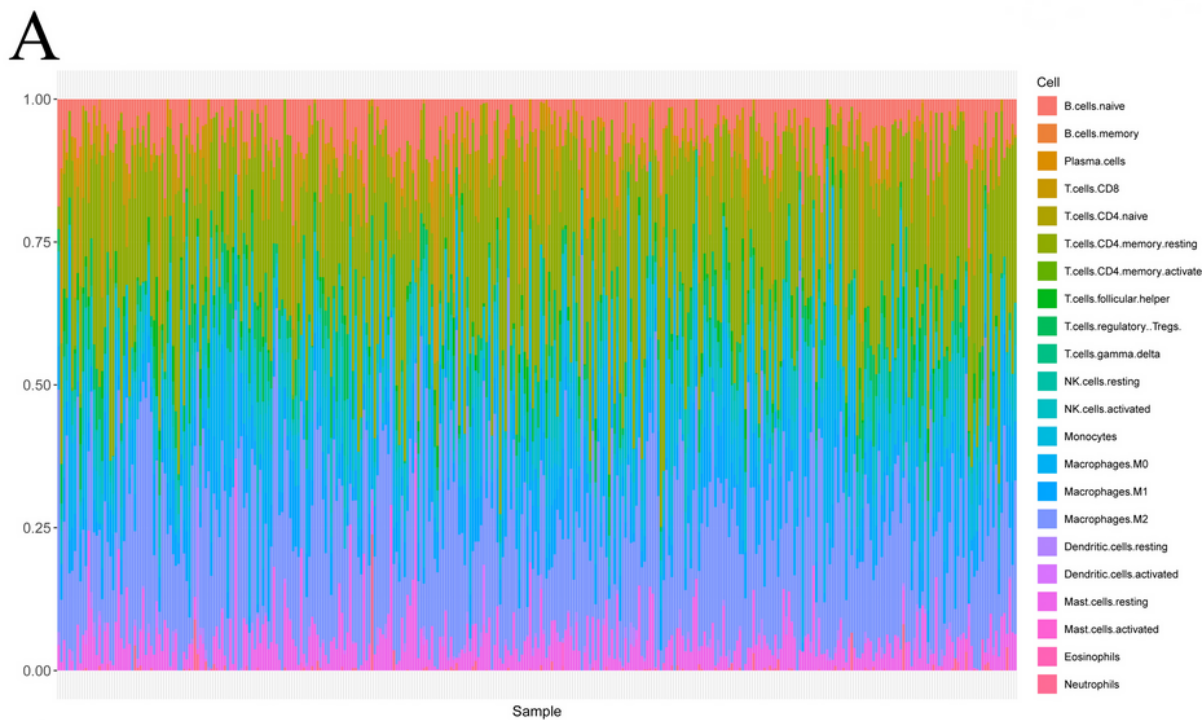
**Figure 3**

Risk score is an independent prognostic marker for HCC. (A) Multivariate Cox regression analysis forest plot. Compared with reference samples, samples with Hazard ratio greater than 1 have a higher risk of death, and samples with Hazard ratio less than 1 have a lower risk of death risk of death. (B -C) Kaplan Meier survival curve of HCC patients  $\leq 60$  years old and  $>60$  years old.



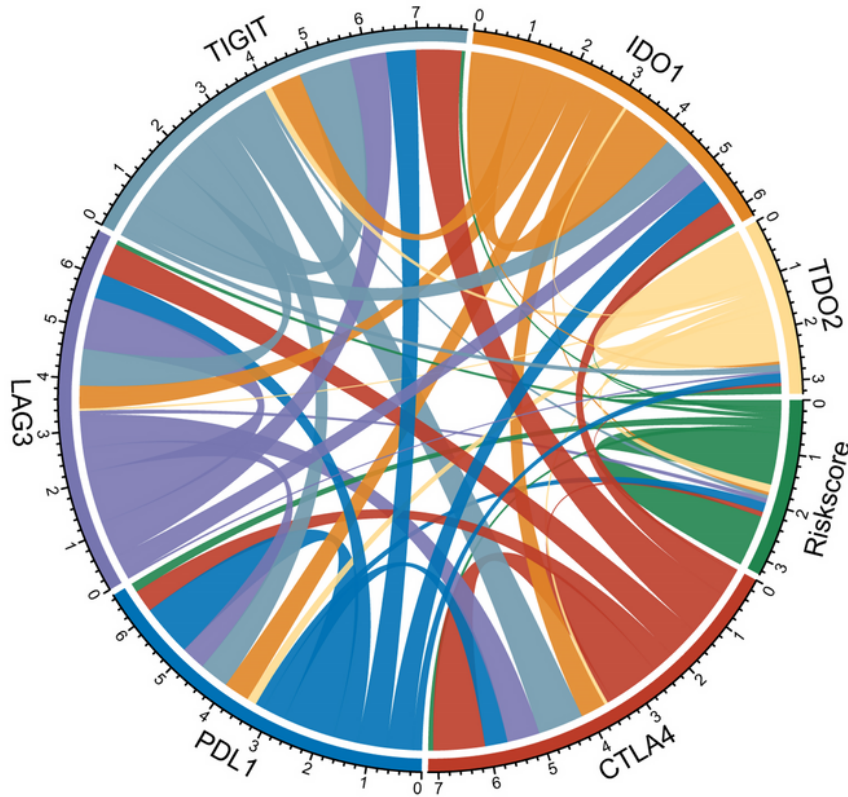
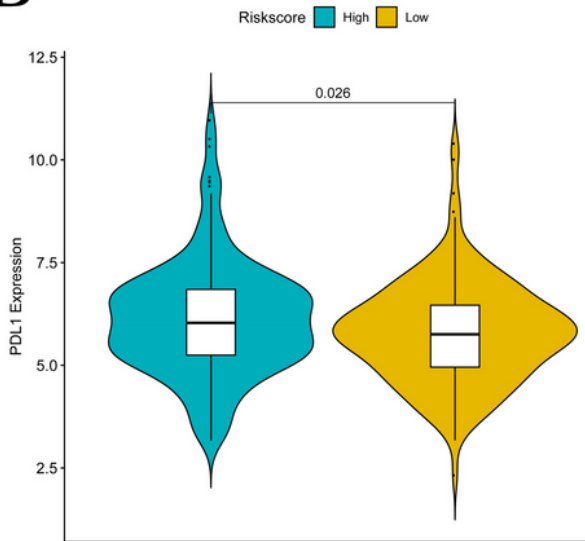
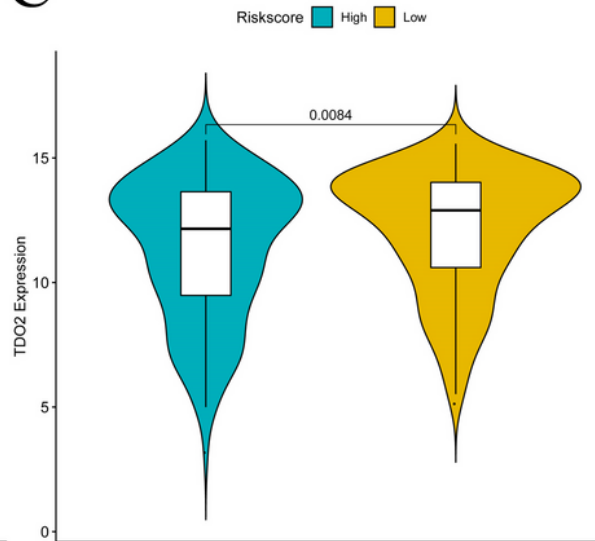
**Figure 4**

Nomogram predicts survival in patients with HCC. (A) Nomogram predicts the probability of OS at 1, 3, and 5 years in patients with HCC. (B-D) Nomogram is a calibration curve for predicting the probability of OS in HCC patients at 1, 3 and 5 years. The X axis represents the nomogram predicted survival rate, and the Y axis represents the actual survival rate.



**Figure 5**

Immune infiltration of HCC patients in the high and low-risk groups. (A) The relative proportion of immune infiltrating cells in all patients. (B) The violin diagram of immune cells with significant difference in high and low-risk group. The horizontal axis represents high and low-risk group, the vertical axis represents relative infiltration ratio of immune cells respectively. The P-value is calculated by wilcoxn method.

**A****B****C****Figure 6**

The relationship between several important immune checkpoints and risk score. (A) Chord diagram of the correlation between the risk score and the expression of the 6 prominent immune checkpoints. The wider the line between them, the stronger the correlation between them. (B-C) The violin chart for PDL1, TDO2 and risk score. Different color indicates the high and low-risk group, while the vertical axis indicates the expression quantity. The P-value is calculated by wilcoxn method.